

# Chapter 7

## Superwicking Surfaces Produced by Femtosecond Laser

A. Y. Vorobyev and Chunlei Guo

**Abstract** Modifying material wetting properties using femtosecond laser surface nano/microstructuring has recently become an actively studied area due to many promising applications. In this chapter, we overview briefly the newly emerged femtosecond laser-based approaches for modifying the wetting properties of materials and describe recent developments in producing a novel type of surface structures that transform a regular surface of solids to superwicking. This novel type of the surface structure is an array of parallel nanostructured microgrooves. In a gravity defying way, water runs vertically uphill on the created superwicking surfaces. The fast self-propelling motion of the liquid is due to strong capillary force generated in the surface structure. The unique wetting and wicking properties of these novel materials may find a wide range of applications in nano/microfluidics, optofluidics, lab-on-chip technology, fluidic microreactors, chemical sensors, biomedicine, and heat transfer devices (e.g., heat pipes for cooling of electronic devices).

### 7.1 Introduction

In nature, there are numerous examples of biological materials with remarkable wetting properties due to surface nano/microstructures. Examples are the leaves of water-repellent plants such as Lotus (*Nelumbo nucifera*) and Lady's mantle (*Alchemilla mollis*), which are superhydrophobic due to a combination of micro- and nano-structures on the surface of their leaves [1, 2]. Due to their superhydrophobicity, these plants have self-cleaning properties, known as "Lotus effect". When water drops roll over the leaves, they pick up dust particles and remove them when rolling off the leaves. Another example is the surface nano/microstructures on the wings of the Morpho butterfly that have two wonderful functions, the generation of the structural blue color and making the wing surface superhydrophobic/self-cleaning similar to Lotus plant [3].

---

A. Y. Vorobyev (✉) · C. Guo

The Institute of Optics, University of Rochester, Rochester, NY 14627, USA  
e-mail: vorobyev@optics.rochester.edu

© Springer Science+Business Media Dordrecht 2015  
O. Shulika, I. Sukhoivanov (eds.), *Advanced Lasers*,  
Springer Series in Optical Sciences 193, DOI 10.1007/978-94-017-9481-7\_7

Surface morphology of a solid is a factor that influences the wetting properties of materials. Modification of wetting properties of materials using surface nano/micro structuring has been extensively studied in the past [4–8]. Traditionally, surface textures for altering the wetting properties are prepared using photolithography [8], electron beam lithography [9], wet chemical etching [10], and plasma techniques [11]. Recently, a new approach based on femtosecond laser surface nano/microstructuring has been developed for modifying the wetting properties of various materials [12–17]. This novel approach has become an active research area due to a number of advantages and many promising applications. The advantages of the femtosecond laser approach include: (i) ability to process a large variety of materials (metals, semiconductors, glasses, and polymers), (ii) simplicity, and (iii) capability to process complicated shapes with the size of the textured surface area as small as a tightly focused laser spot, i.e., down to about 10  $\mu\text{m}$ , or as large as needed when a raster scanning of the laser beam is used.

Modification of wetting properties using femtosecond laser has been first demonstrated in Refs. [12, 13], where silicon wafers were treated with high-intensity ultrashort laser pulses in  $\text{SF}_6$  environment to produce quasi-ordered arrays of conical microspikes. Following the laser surface treatment, Zorba *et al.* [13] produced superhydrophobic silicon. A water contact angle as high as  $160^\circ$  was reported. The authors of Ref. [12] produced superhydrophobic silicon by coating the conical microspikes with a layer of fluoroalkylsilane molecules. The authors of Refs. [18, 19] have found that depositing various functional coatings on the laser-nano/microstructured silicon allows producing engineered surfaces with wetting properties that can be changed by external stimuli (light, electric field, and  $\text{pH}$ ). Effects of various surface textures induced by femtosecond laser pulses on wetting properties of platinum has been studied in [14]. The studied surface textures included irregular nanostructures, periodic surface structures, and hierarchical structures (combinations of nano- and micro-structures). It has been found that laser-structured surfaces become hydrophobic or even superhydrophobic for some textures. For example, a water contact angle as high as  $158^\circ$  was observed on the hierarchical surface structures. A detailed study of the wetting properties of stainless steel and titanium alloy following femtosecond laser surface structuring has been performed in [15]. It was observed that the treated surfaces are hydrophilic immediately after femtosecond laser processing but subsequently become superhydrophobic with time. The dramatic change in wetting behavior was attributed to accumulation of carbon on the laser-treated surface. The authors of Ref. [20] have studied the wetting properties of polymethyl methacrylate (PMMA) following femtosecond laser ablation. In this study, both hydrophilic and hydrophobic surfaces were produced depending on laser fluence. The hydrophobic surfaces were generated at a low laser fluence between 0.4 and 2.1  $\text{J}/\text{cm}^2$ , while hydrophilic surfaces were produced at a laser fluence in the range of 2.1–52.7  $\text{J}/\text{cm}^2$ . Different wetting behavior of the laser-treated PMMA was explained by laser-induced chemical bond changes, not to the produced surface texture. A superhydrophobic surface texture on poly(dimethylsiloxane) (PDMS) following femtosecond laser processing has been reported in Ref. [21]. The fabricated superhydrophobic surface had a contact angle higher than  $170^\circ$  and sliding angle less than  $3^\circ$ .

The authors of Ref. [22] altered initially hydrophilic surface of polyethersulfone to superhydrophobic through femtosecond laser-induced both structural and chemical modifications.

Recently, novel superwicking surfaces have been created using direct femtosecond laser writing. These novel materials can make liquids run vertically uphill against the gravity over an extended surface area. Furthermore, they exhibit superhydrophilic and superwetting properties. The unique wetting and wicking properties of these novel materials may find a wide range of applications in thermal management, nano/microfluidics, optofluidics, lab-on-chip technology, fluidic microreactors, chemical sensors, and biomedicine. In this chapter, we overview the recent developments in producing superwicking surfaces and describe their potential applications.

## 7.2 Basic Idea of Wicking Structures and Their Fabrication Using Femtosecond Laser

The creation of superwicking structures using a femtosecond laser has been previously reported in [16, 23, 24]. The basic idea of wicking structures produced in [16, 23, 24] is as follows. The capillary effect in a pipe is a well known phenomenon demonstrated in Fig. 7.1a. A much less known fact is that the capillary force is also generated in a half-pipe as illustrated in Fig. 7.1b. Therefore, through engraving an array of parallel microgrooves on a surface of a solid, one can fabricate a wicking (capillary) surface of a large area as schematically shown in Fig. 7.1c. However, the capillary force in the half-pipe is much smaller than in the pipe [25]. Therefore, for enhancing the capillary action in the microgrooves, the authors of Refs. [16, 23, 24] used femtosecond laser nanostructuring of the surface of the microgrooves. The mechanism of enhancing the capillary action in the microgrooves through nanostructuring of their surface is explained as follows. It is known that the capillary action of various capillary systems depends on the hydrophilicity of the surface that is in contact with the liquid. For example, the maximum capillary rise of a liquid in the tube is given by [26]

$$h = \frac{2\gamma \cos \theta}{\rho g R} \quad (7.1)$$

where  $\gamma$  is the liquid-air surface tension,  $\theta$  is the contact angle,  $\rho$  is the density of liquid,  $g$  is the gravitational acceleration, and  $R$  is the tube radius. The formula (7.1) shows that the smaller the contact angle  $\theta$  (the higher hydrophilicity), the stronger the capillary action.

Following the Wenzel model, the wetting of a rough surface is described by relation [4]

$$\cos \theta^* = r \cos \theta \quad (7.2)$$

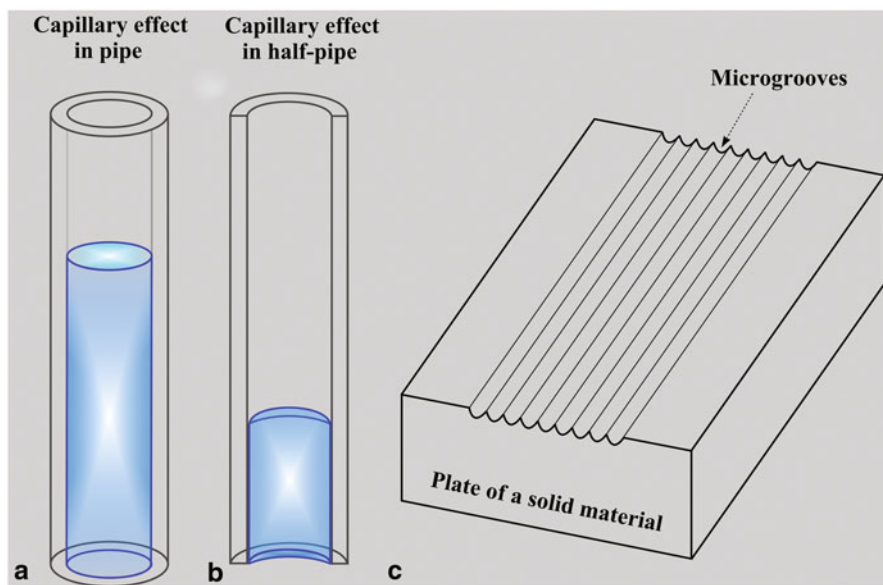


**Fig. 7.1** Basic idea of producing the wicking (capillary) surfaces

where  $\theta^*$  is the apparent contact angle on a rough surface,  $r$  is the roughness factor (the ratio of the actual surface area to the geometrically projected area on the horizontal plane), and  $\theta$  is the contact angle on a smooth horizontal surface of the same material (Young contact angle). Since  $r$  is always greater than 1, the surface texture enhances the hydrophilicity of an originally hydrophilic surface ( $\theta < 90^\circ$ ) and enhances the hydrophobicity of an originally hydrophobic surface ( $\theta > 90^\circ$ ). Since the materials used in capillary systems are intrinsically hydrophilic, the texturing of the surfaces that are in contact with the liquid will enhance the hydrophilicity (reduce the contact angle  $\theta$ ) and thereby will enhance the capillary action. Over the last few years, the direct femtosecond laser surface nano/microstructuring has been established as a versatile approach for controllable producing a large variety of surface structures at nano- and micro-scales on metals, semiconductors, glasses, polymers, and other materials [27–43]. Therefore, the femtosecond laser is a very efficient tool for producing the microgrooves with nanostructured surface. A typical setup used for producing the capillary microgrooves with nanostructured surface is shown in Fig. 7.2. Pulses from a femtosecond laser are focused by a lens onto a sample mounted on a computer-controlled XY-translation stage. A beamsplitter and joulemeter are used for monitoring the femtosecond laser pulse energy. An electromechanical shutter is used to block the laser beam in raster scanning. A neutral density filters are used to vary laser fluence incident on the sample. The femtosecond laser setup shown in Fig. 7.2 is suitable for producing a single microgroove when sample is translated along the X- or Y-axis, or an array of parallel microgrooves over

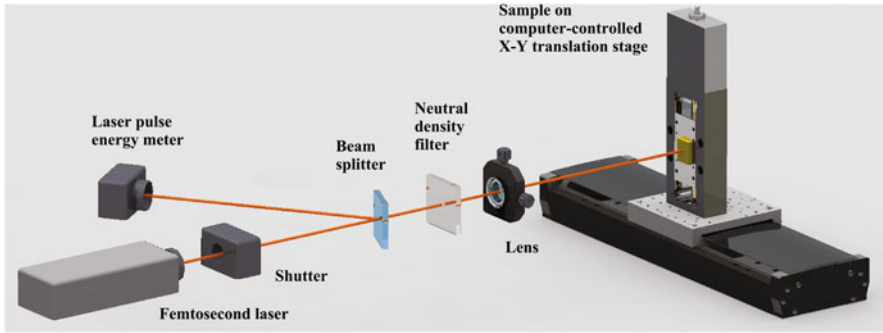


**Fig. 7.2** Typical experimental setup for producing microgrooves on the surface of solids

a large surface area when the sample is raster scanned. By varying the parameters of the laser pulses incident upon the treated metal, the microgroove geometry can be controlled. Commonly, the capillary microgrooves are produced in two steps. In the first step, the microgrooves are produced using high laser fluence. In the second step, the microgrooves surface is then nanostructured using low or moderate laser fluence for achieving a maximum enhancement of the hydrophilicity. For some materials, even one-step processing can be sufficient for producing efficient capillary microchannels due to nanostructures commonly left on the microgroove surface after processing at high laser fluence. In the following section, we discuss the capillary action of femtosecond laser fabricated superwicking structures.

### 7.3 Spreading of Liquids on Superwicking Surfaces

Glass is a widely used material in microfluidics, optofluidics, lab-on-chip technology, and biomedical devices [44–46]. Although the glass is a transparent material, it can be easily processed using tightly focused femtosecond laser pulses due to nonlinear absorption of high-intensity light [47]. Figure 7.3a shows a photograph of the femtosecond laser treated glass sample, where the superwicking structure is an array of parallel microgrooves with a nanostructured surface. Figure 7.3b shows a 3D optical image of the treated surface, where we can see that the microgroove period, depth, and width are about 100, 32, and 28  $\mu\text{m}$ , respectively. Figure 7.3c and 7.3d show the details of the surface structural features. One can see that the surface of both ridges and valleys of the microgrooves has engraved nano- and fine micro-structures. Figure 7.3d shows that the laser-induced nanostructures include both nanoprotusions and nanocavities, while fine microstructures include microcavities and microscale aggregates composed of nanoparticles that fuse onto each other and on the glass surface. The average size of superimposed fine microstructures is about 2.7  $\mu\text{m}$ .

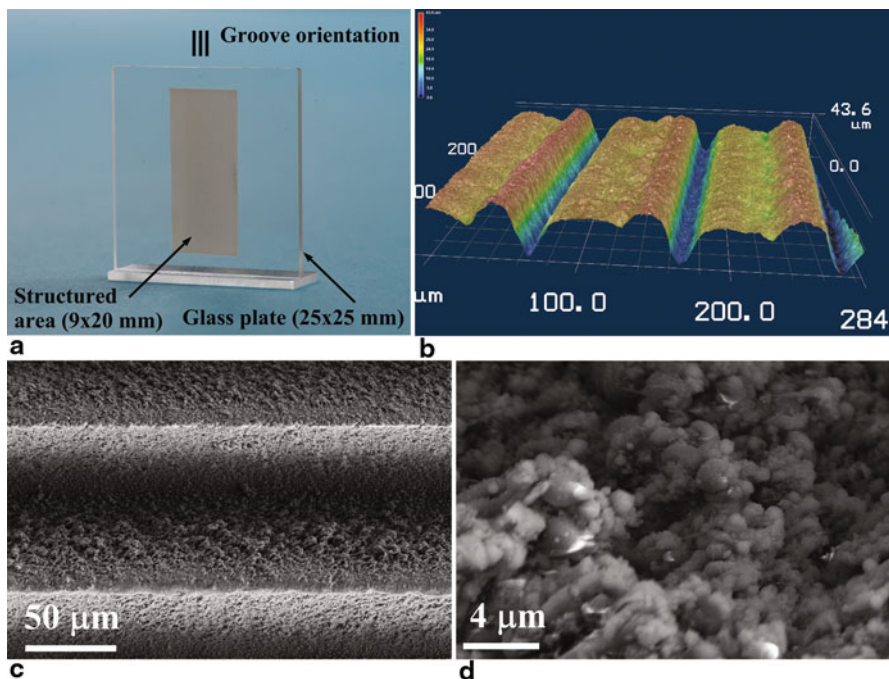


**Fig. 7.3** **a** Photograph of the femtosecond laser treated glass sample. **b** A 3D optical image of the surface capillary microgrooves. **c** and **d** fine micro- and nano-structural features on the microgrooves [24]

The capillary action of the sample shown in Fig. 7.3 is demonstrated in Figs. 7.4 and 7.5. Figure 7.4 shows the spreading dynamics of a 3- $\mu\text{l}$  water droplet deposited on the horizontally-positioned structured glass surface. For a comparison, the behavior of a 3- $\mu\text{l}$  water droplet deposited on an untreated glass surface is also shown in Figs. 7.4a, 7.4b, 7.4c, 7.4d, 7.4e, 7.4f. Figure 7.4 shows that the water spreading is highly anisotropic on the treated area and it occurs preferentially along the microgrooves. One can deduce from Fig. 7.4b that average initial velocity of water front spreading is about 5.8 cm/s within the first 0.2 s. However, the spreading velocity decreases with time, as seen from Figs. 7.4c, 7.4d, 7.4e, 7.4f. The experiments with different volumes of water in the range of 1–6  $\mu\text{l}$  show the similar highly anisotropic spreading behavior. Figure 7.5 shows the spreading dynamics of a 3- $\mu\text{l}$  water droplet pipetted on the vertically-positioned glass sample with the microgrooves oriented vertically. The snapshots of water spreading shown in Figs. 7.5a, 7.5b, 7.5c, 7.5d, 7.5e, 7.5f demonstrate that the water deposited on the bottom of the groove area immediately sprints vertically uphill against the gravity. It is seen that this gravity-defying uphill motion easily extends over several centimeters. This experiment clearly demonstrates that the femtosecond laser processing makes a regular glass surface to be superwicking, with a driving force much stronger than the

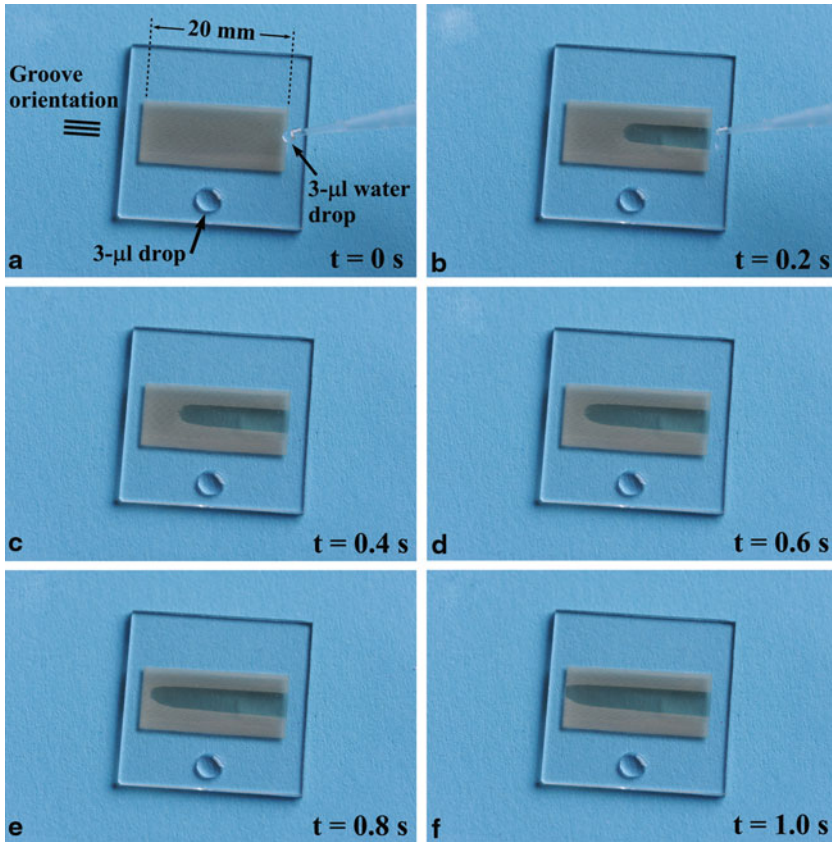


**Fig. 7.4** Spreading dynamics of water on a horizontally-positioned glass sample. The average water spreading velocity is about 3.8 cm/s within the first 0.2 s and it reduces to about 2 cm/s for the time interval of 1 s [24]

gravity. One can deduce from Fig. 7.5b, that the average water front spreading velocity is about 3.8 cm/s within the first 0.2 s, and this velocity is lower than the water spreading along the horizontal grooves in Fig. 7.4b. As seen in Figs 7.5a, 7.5b, 7.5c, 7.5d, 7.5e, 7.5f, the spreading velocity decreases with time similar to the case of horizontal orientation of the microgrooves (Figs. [4], 7.4b, 7.4c, 7.4d, 7.4e, 7.4f).

In the past, fluid flow has been studied in various capillary systems such as tubes, open surface grooves, and two-dimensional arrays of pillars. It has been shown by Washburn [48] that flowing of a wetting liquid in a capillary tube follows a diffusion law as  $z(t) \propto (Dt)^{1/2}$ , where  $z$  is the distance traveled by the liquid,  $t$  is the time, and  $D$  is the diffusion constant. Spreading of wetting fluids has been also studied in open capillary systems, such as surface grooves [49–52] and two-dimensional arrays of pillars [6, 8]. It has been shown that the spreading dynamics in open V-shaped

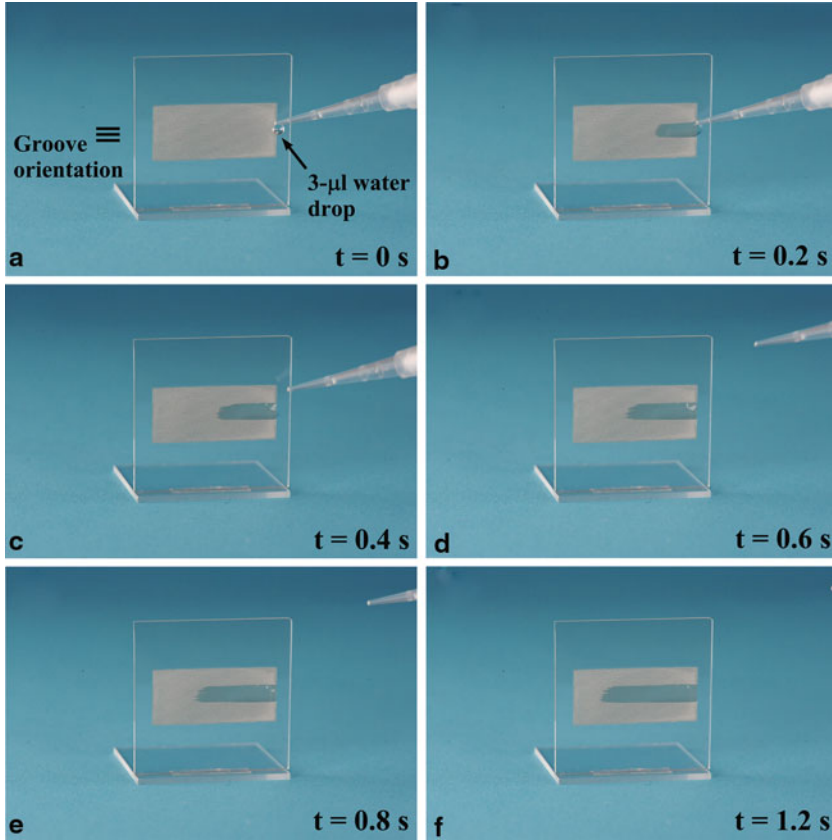


**Fig. 7.5** Dynamics of water running uphill against the gravity on a vertically-standing glass sample with grooves oriented vertically. **a–f** Snapshots of water spreading vertically uphill with time [24]

grooves also follows the  $t^{1/2}$  dependence [50]

$$z^2 = K(\alpha, \theta)[\gamma h_0 / \mu]t \quad (7.3)$$

where  $K(\alpha, \theta)$  is the geometry term with  $\alpha$  and  $\theta$  being the groove angle and the contact angle,  $\gamma$  and  $\mu$  are the surface tension and viscosity of the liquid, and  $h_0$  the groove depth. The authors of Refs. [6, 8] have demonstrated that the Washburn-type dynamics also holds on surfaces textured with regular arrays of pillars. There is a general consensus that a structured surface can be viewed as a network of open capillaries, where the liquid spreading from a reservoir usually follows the Washburn-type scaling law  $z \propto (Dt)^{1/2}$  [6, 8, 49, 50, 53, 54]. In contrast to previously studied open grooves, the surface of the open grooves produced by ultrafast laser has a highly hierarchical structure. Figure 7.6 shows a plot of the uphill travel distance  $z$  as a function of  $t^{1/2}$  for the vertically standing glass sample shown in Fig. 7.5. It is



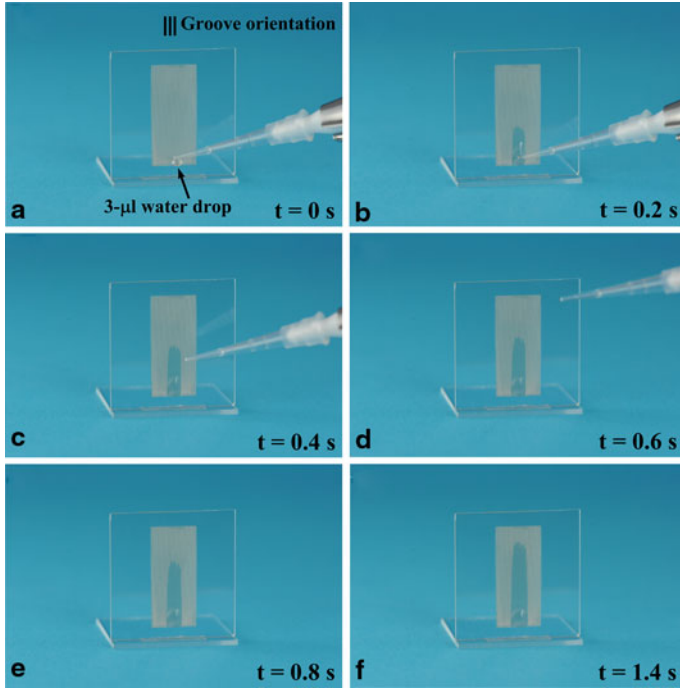


**Fig. 7.6** Uphill distance traveled by water front as a function of  $t^{1/2}$  [24]

seen that the water spreading distance linearly depends on  $t^{1/2}$  despite of extremely sophisticated surface topology. This observation indicates that the Washburn-type  $t^{1/2}$  dynamics is indeed universal for the various capillary systems. The structure of the open capillary systems produced by femtosecond laser [16, 23, 24] can be considered as composed of two substructures: (1) an array of microgrooves and (2) irregular structures on nano- and fine micro-scales superimposed on the surface of the microgrooves. Therefore, the capillary action of the laser-produced open capillary systems is a combined capillary effect from both substructures. Thus, the texture on the microgroove surface plays two roles. First, it enhances the hydrophilicity of the microgroove surface. Second, it generates its own capillary flow. Previously, Bico et al. [55] have modeled capillary rise in a tube with a surface textured by a designed regular roughness. Their model predicts two different capillary rises in a tube decorated with regular spikes: one inside the entire volume of the tube and the other only inside the spikes. The liquid spreading in the spikes forms a film that spreads faster than the main meniscus, causing a broadening of the liquid front. Is this also holds for femtosecond laser produced open microgrooves is not yet studied.

At present, the superwicking effect has been demonstrated for a number of solid materials, including glass, silicon, metals, and biological hard tissues [16, 23, 24, 56, 57]. Recently, wicking surfaces have been produced using nanosecond laser pulses [58].

## 7.4 Potential Applications of Capillary Superwicking Structures

Areas of potential applications of the capillary superwicking materials produced by femtosecond laser processing include cooling devices, nano/microfluidics, optofluidics, lab-on-chip technology, fluid microreactors, biomedicine, and biochemical sensors. Below, we give a short overview of some applications.

As devices and components in electronics, telecommunication, and computers become smaller and smaller, the demand for miniaturized high-performance cooling systems becomes important. Currently, the heat flux at both the chip and module levels of packaging can be so high ( $> 1000 \text{ W/cm}^2$ ) that it exceeds the practical limit of the traditional air-cooling. To combat this problem, microfluidic cooling of the chips is actively pursued. Tuckerman and Pease [59] have demonstrated that a microchannel heat sink integrated into a silicon chip is capable of dissipating a circuit power density of  $790 \text{ W/cm}^2$ . Presently, the microchannels in IC microfluidic heat sinks are commonly fabricated using deep reactive ion etching. One can expect that the laser fabricated capillary channels with textured surfaces will enhance the cooling performance of microchannel heat sinks by optimizing both nanostructure-induced turbulences in the microchannels and surface wettability. Cooling through liquid-vapor phase transition is potentially the most efficient way to dissipate high heat flux due to a high latent heat of the liquid-vapor phase transition. In the case of two-phase (flow boiling) microfluidic cooling, the superwicking microchannels can improve the cooling performance through larger surface area, enhancing fresh liquid refilling of the vapor bubble voids, and enhancing prevention of dry-out spots. Furthermore, the superwicking microchannels can find applications in miniature heat pipes for returning the working liquid from the condenser back to the evaporator.

In microfluidic systems, a pump is the most expensive and complicated component with a high failure rate. Therefore, passive microfluidic systems, where fluids are driven by capillary wicking action, are beneficial. The strong capillary action of the microchannels fabricated by the femtosecond laser [16, 23, 24] is a promising way to produce efficient capillary-driven microfluidic-based devices. Furthermore, this technique is promising for the fabrication of various other microfluidic components. For example it can be used for fabricating T- and Y-micromixers, where the microchannels with bas-relief structures, such as ribs [60] and staggered-herringbone grooves [61] on the floor and walls, are used for enhanced mixing of solutions in the microchannels through enhancing chaotic advection. Another potential application of this novel laser technique is the fabrication of capillary-driven microvalves that are used in microfluidic biochemical devices for stopping and delaying fluids in the microchannels. Operation of these passive capillary microvalves is based on an abrupt change in the geometry and wetting properties of the capillary microchannels [62, 63]. The femtosecond laser technology can be also used for fabricating separators [64] and capillary pumps [65]. Moreover, this laser technology has a great potential for the fabrication of superior autonomous microfluidic capillary sensing systems, where all required operations (pumping, valving, separating, and synchronization) are capillary-driven, without any external actuators [66]. Since the femtosecond laser technology of producing microfluidic systems and their components can be easily

integrated into a Computer Numerical Control (CNC) laser machine, this technology is attractive from a commercialization point of view.

Good wettability of enamel and dentin surfaces is desirable in enhancing adhesion of restorative materials in dentistry. At the present time, surface texturing of the enamel and dentin surfaces through etching with an acidic or basic solution for improving the wettability is a widely used approach in adhesive dentistry. In contrast to the traditional chemical etching that produces random surface roughness, the authors of Ref. [57] developed a new approach, which is based on producing engineered surface structures using the femtosecond laser surface nano/microstructuring technique. The engineered surface structure consists of an array of parallel microgrooves that generate a strong capillary force. Figure 7.7a shows the photograph of the femtosecond laser treated dentin specimen. The 3D optical image of the array of microgrooves produced on the dentin specimen is shown in Fig. 7.7b. Fine structural details of the microgroove surface are shown in Fig. 7.7c and 7.7d. The water contact angle before the laser treatment was measured to be  $42^\circ$  and  $48^\circ$  on the enamel and dentin specimens, respectively. After laser treatment, the contact angle on the laser-treated surface was measured to be  $\sim 0^\circ$  for both the enamel and dentin specimens. This means that the treated surfaces are superwetting [67]. The superwetting behavior can be seen from Figs. 7.7e and 7.7f, where a  $1\ \mu\text{l}$  water droplet sprints vertically uphill on a vertically standing laser-treated dentin surface. From these snapshots, the average water spreading velocity on the vertical dentin surface can be deduced to be about  $21.7\ \text{mm/s}$  within the first  $0.2\ \text{s}$ . From practical point of view, this means that wetting occurs instantaneously. The method reported in Ref. [57] for controllable enhancement of the wettability can be extended to human bones (because both the human teeth and bones are mainly composed of hydroxyapatite) and can be also used for the hydroxyapatite coatings of implants. This method for modifying the wettability is also suitable for a variety of biocompatible materials used in dentistry, medicine, biomedicine, and biosensing.

## 7.5 Conclusions

Over the past 7 years, significant progress has been made in applying femtosecond laser nano/microstructuring technology to alter the wetting properties of materials. It has been found that this approach is also capable of producing superwicking materials. The surface structure of these materials is an array of parallel microgrooves extensively covered by nano- and micro-scale structures. The capillary action of the created superwicking surfaces is so strong that the treated surfaces can make liquids run vertically uphill over an extended surface area. The wicking dynamics follows the classical square root of time dependence despite of a very complex geometry of the created wicking surface structure. The superwicking effect has been demonstrated on a number of solid materials, including glass, silicon, metals, and biological hard tissues. The femtosecond laser technology is suitable for processing complicated surface shapes at various dimensions. In contrast to commonly used surface

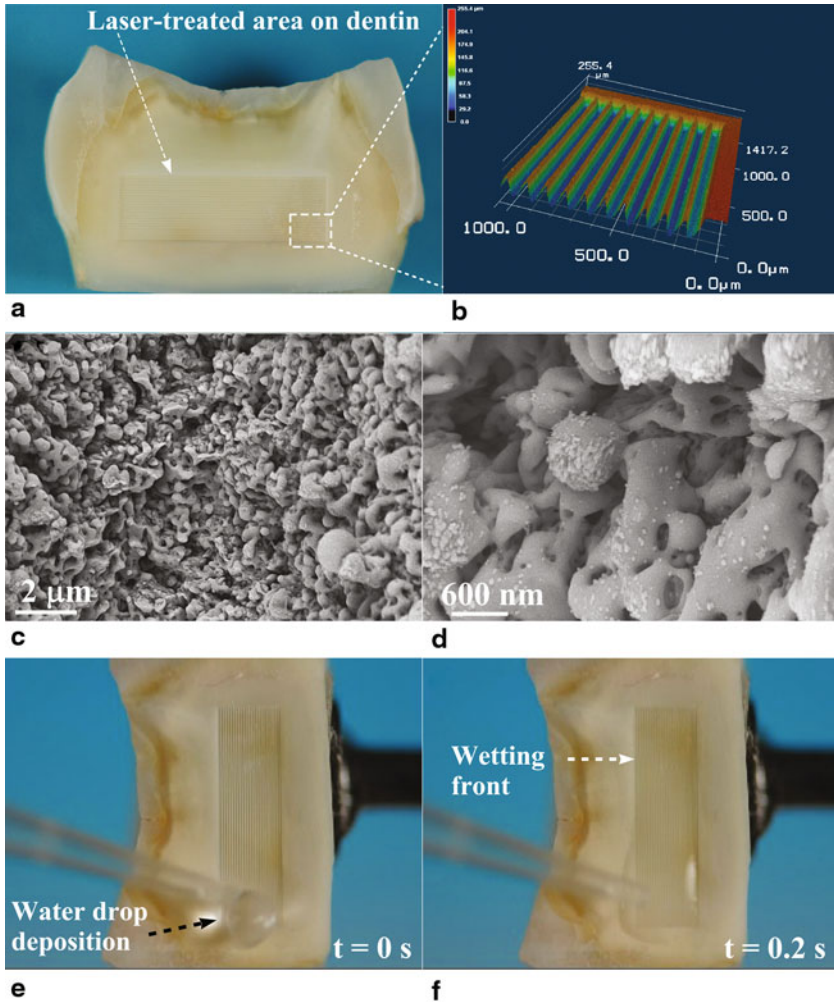


**Fig. 7.7** **a** Photograph of a tooth with a laser-treated area on the dentin surface (a surface area textured with the microgroove pattern is 2.2 (6 mm<sup>2</sup>). **b** 3D optical image of the laser-produced microgrooves. **c** and **d** SEM images showing fine micro- and nano-roughness on the surface of the microgrooves. **e** and **f** Water spreading on the laser-treated dentin surface positioned vertically [57]

lithography techniques, the laser processing does not utilize chemical etchants and is therefore free of chemical contamination. The superwicking materials produced by femtosecond laser processing may find a wide range of applications in chromatography, nano/microfluidics, optofluidics, cooling devices, lab-on-chips, biomedicine, biochemical sensors, and fluid microreactors.

**Acknowledgements** This work was supported by the Bill & Melinda Gates Foundation.

## References

1. Barthlott, W., Neinhuis, C.: Purity of the sacred lotus, or escape from contamination in biological surfaces. *Planta* **202**(1), 1–8 (1997)
2. Otten, A., Herminghaus, S.: How plants keep dry: a physicist's point of view. *Langmuir* **20**(6), 2405–2408 (2004)
3. Gu, Z.Z., Uetsuka, H., Takahashi, K., Nakajima, R., Onishi, H., Fujishima, A., Sato, O.: Structural color and the lotus effect. *Angew. Chem. Int. Ed.* **42**(8), 894–897 (2003)
4. Wenzel, R.N.: Resistance of solid surfaces to wetting by water. *Ind. Eng. Chem.* **28**(8), 988–994 (1936)
5. Cassie A.B.D., Baxter S.: Wettability of porous surfaces. *Trans. Faraday Soc.* **40**, 546–551 (1944)
6. Bico, J., Tordeux, C., Quere, D.: Rough wetting. *Europhys. Lett.* **55**(2), 214–220 (2001)
7. McHale, G., Shirtcliffe, N.J., Aqil, S., Perry, C.C., Newton, M.I.: Topography driven spreading. *Phys. Rev. Lett.* **93**(3), 036102 (2004)
8. Courbin, L., Deniel, E., Dressaire, E., Roper, M., Ajdari, A., Stone, H.A.: Imbibition by polygonal spreading on microdecorated surfaces. *Nat. Mater.* **6**, 661–664 (2007)
9. Martines, E., Seunarine, K., Morgan, H., Gadegaard, N., Wilkinson, C.D.W., Riehle, M.O.: Superhydrophobicity and superhydrophilicity of regular nanopatterns. *Nano Lett.* **5**(10), 2097–2103 (2005)
10. Wang, Q., Zhang, B.W., Qu, M.N., Zhang, J.Y., He, D.Y.: Fabrication of superhydrophobic surfaces on engineering material surfaces with stearic acid. *Appl. Surf. Sci.* **254**(7), 2009–2012 (2008)
11. Woodward, I., Schofield, W.C.E., Roucoules, V., Badyal, J.P.S.: Super-hydrophobic surfaces produced by plasma fluorination of polybutadiene films. *Langmuir* **19**(8), 3432–3438 (2003)
12. Baldacchini, T., Carey, J.E., Zhou, M., Mazur, E.: Superhydrophobic surfaces prepared by microstructuring of silicon using a femtosecond laser. *Langmuir* **22**(11), 4917–4919 (2006)
13. Zorba, V., Persano, L., Pisignano, D., Athanassiou, A., Stratakis, E., Cingolani, R., Tzanetakis, P., Fotakis, C.: Making silicon hydrophobic: wettability control by two-lengthscale simultaneous patterning with femtosecond laser irradiation. *Nanotechnology* **17**(13), 3234–3238 (2006)
14. Fadeeva, E., Schlie, S., Koch, J., Chichkov, B.N., Vorobyev, A.Y., Guo, C.: Femtosecond laser-induced surface structures on platinum and their effects on hydrophobicity and fibroblast cell proliferation. In: Mittal, K.L. (ed.) *Contact Angle, Wettability And Adhesion*, vol. 6, pp. 163–171. VSP/Brill, Leiden (2009)
15. Kietzig, A.M., Hatzikiriakos, S.G., Englezos, P.: Patterned superhydrophobic metallic surfaces. *Langmuir* **25**(8) 4821–4827 (2009)
16. Vorobyev, A.Y., Guo, C.: Metal pumps liquid uphill. *Appl. Phys. Lett.* **94**(22), 224102 (2009).
17. Kruse, C., Anderson, T., Wilson, C., Zuhlke, C., Alexander, D., Gogos, G., Ndao, S.: Extraordinary shifts of the Leidenfrost temperature from multiscale micro/nanostructured surfaces. *Langmuir* **29**(31), 9798–9806 (2013)
18. Papadopoulou, E.L., Barberoglou, M., Zorba, V., Manousaki, A., Pagkozidis, A., Stratakis, E., Fotakis, C.: Reversible photoinduced transition of hierarchical ZnO structures. *J. Phys. Chem. C* **113**(7), 2891–2895 (2009)
19. Stratakis, E., Ranella, A., Fotakis, C.: Biomimetic micro/nanostructured functional surfaces for microfluidic and tissue engineering applications. *Biomicrofluidics* **5**(1), 013411 (2011)
20. Wang, Z.K., Zheng, H.Y., Lim, C. P., Lam, Y.C.: Polymer hydrophilicity and hydrophobicity induced by femtosecond laser direct irradiation. *Appl. Phys. Lett.* **95**(11), 111110 (2009)

21. Yoon, T.O., Shin, H.J., Jeoung, S.C., Park, Y. I.: Formation of superhydrophobic poly(dimethylsiloxane) by ultrafast laser-induced surface modification. *Opt. Express*. **16**(17), 12715–12725 (2008)
22. Pazokian, H., Selimis, A., Barzin, J., Jelvani, S., Mollabashi, M., Fotakis, C., Stratakis, E.: Tailoring the wetting properties of polymers from highly hydrophilic to superhydrophobic using UV laser pulses. *J. Micromech. Microeng.* **22**(3), 035001 (2012)
23. Vorobyev, A.Y., Guo, C.: Laser turns silicon superwicking. *Opt. Express*. **18**(7), 6455–6460 (2010)
24. Vorobyev, A.Y., Guo, C.: Superwicking glass produced by femtosecond laser. *J. Appl. Phys.* **108**, 123512 (2010)
25. Raphael, E.: Capillary rise of a wetting fluid in a semi-circular groove. *J. Phys. France*. **50**(4), 485–491 (1989)
26. Batchelor, G.K.: An introduction to fluid dynamics. Cambridge University Press (1967)
27. Vorobyev, A.Y., Guo, C.: Enhanced absorbance of gold following multi-pulse femtosecond laser ablation. *Phys. Rev. B* **72**(19), 195422 (2005)
28. Vorobyev, A.Y., Guo, C.: Femtosecond laser nanostructuring of metals. *Opt. Express*. **14**(6) 2164–2169 (2006)
29. Vorobyev, A.Y., Guo, C.: Femtosecond laser structuring of titanium implants. *Appl. Surf. Sci.* **253**(17), 7272–7280 (2007)
30. Zhakhovskii, V.V., Inogamov, N. A., Nishihara, K.: New mechanism of the formation of the nanorelief on a surface irradiated by a femtosecond laser pulse. *JETP Lett.* **87**(8), 423–427 (2008)
31. Zavestovskaya, I.N., Kanavin, A.P., Men'kova, N.A.: Crystallization of metals under conditions of superfast cooling when materials are processed with ultrashort laser pulses. *J. Opt. Technol.* **75**(6), 353–358 (2008)
32. Stratakis, E., Zorba, V., Barberoglou, M., Fotakis, C., Shafeev, G.: Laser writing of nanostructures on bulk Al via its ablation in liquids. *Nanotechnology*. **20**(10), 105303 (2009)
33. Barmina, E.V., Barberoglu, M., Zorba, V., Simakin, A.V., Stratakis, E., Fotakis, C., Shafeev, G.A.: Surface nanotexturing of tantalum by laser ablation in water. *Quantum Electron.* **39**(1), 89–93 (2009)
34. Barmina, E.V., Stratakis, E., Fotakis, C., Shafeev, G.A.: Generation of nanostructures on metals by laser ablation in liquids: new results. *Quantum Electron.* **40**(11), 1012–1020 (2010)
35. Oliveira, V., Ausset, S., Vilar, R.: Surface micro/nanostructuring of titanium under stationary and non-stationary femtosecond laser irradiation. *Appl. Surf. Sci.* **255**(17), 7556–7560 (2009)
36. Demaske, B.J., Zhakhovsky, V.V., Inogamov, N.A., Oleynik, I.I.: Ablation and spallation of gold films irradiated by ultrashort laser pulses. *Phys. Rev. B*. **82**(6), 064113 (2010)
37. Li, X., Yuan, C., Yang, H., Li, J., Huang, W., Tang, D., Xu, Q.: Morphology and composition on Al surface irradiated by femtosecond laser pulses. *Appl. Surf. Sci.* **256**(13), 4344–4349 (2010)
38. Dai, Y., He, M., Bian, H., Lu, B., Yan, X., Ma, G.: Femtosecond laser nanostructuring of silver film. *Appl. Phys. A*. **106**(3), 567–574 (2012)
39. Zuhlke, C.A., Alexander, D.R., Bruce III, J.C., Ianno, N.J., Kamler, C.A., Yang, W.: Self-assembled nanoparticle aggregates from line focused femtosecond laser ablation. *Opt. Express*. **18**(5), 4329–4339 (2010)
40. Nayak, B.K., Gupta, M.C.: Self-organized micro/nano structures in metal surfaces by ultrafast laser irradiation. *Opt. Lasers Eng.* **48**(10), 940–949 (2010)
41. Hwang, T. Y., Vorobyev, A. Y., Guo, C.: Ultrafast dynamics of femtosecond laser-induced nanostructure formation on metals. *Appl. Phys. Lett.* **95**(12), 123111 (2009)
42. Sivakumar, M., Venkatakrishnan, K., Tan, B.: Characterization of MHz pulse repetition rate femtosecond laser-irradiated gold-coated silicon surfaces. *Nanoscale Res. Lett.* **6**(1), 78 (2011)
43. Vorobyev, A.Y., Guo, C.: Direct femtosecond laser surface nano/microstructuring and its applications. *Laser Photonics Rev.* **7**(3) 385–407 (2013)
44. Psaltis, D., Quake, S.R., Yang, C.: Developing optofluidic technology through the fusion of microfluidics and optics. *Nature*. **442**, 381–386 (2006)

45. Monat, C., Domachuk, P., Eggleton, B. J.: Integrated optofluidics: a new river of light. *Nat. Photonics*, **1**, 106–114 (2007)
46. Tokeshi, M., Minagawa, T., Uchiyama, K., Hibara, A., Sato, K., Hisamoto, H., Kitamori, T.: Continuous-flow chemical processing on a microchip by combining microunit operations and a multiphase flow network. *Anal. Chem.* **74**(7), 1565–1571 (2002)
47. Gattass, R.R., Mazur, E.: Femtosecond laser micromachining in transparent materials. *Nature Photonics*, **2**, 219–225 (2008)
48. Washburn, E.W.: The dynamics of capillary flow. *Phys Rev.* **17**(3), 273–283 (1921)
49. Romero, L.A., Yost, F.G.: Flow in an open channel capillary. *J. Fluid Mech.* **322**, 109–129 (1996)
50. Rye, R.R., Mann, J.A., Yost, F.G.: The flow of liquids in surface grooves. *Langmuir*, **12**(2), 555–565 (1996)
51. Khare, K., Herminghaus, S., Baret, J.-C., Law, B. M., Brinkmann, M., Seemann, R.: Switching liquid morphologies on linear grooves. *Langmuir*, **23**(26), 12997–13006 (2007)
52. Baret, J.-C., Decre, M.M.J., Herminghaus, S., Seemann, R.: Transport dynamics in open microfluidic grooves. *Langmuir*, **23**(9), 5200–5204 (2007)
53. Hay, K.M., Dragila, M.I., Liburdy, J.: Theoretical model for the wetting of a rough surface. *J. Colloid Interface Sci.* **325**(2), 472–477 (2008)
54. Mai, T.T., Lai, C.Q., Zheng, H., Balasubramanian, K., Leong, K.C., Lee, P.S., Lee, C., Choi, W.K.: Dynamics of wicking in silicon nanopillars fabricated with interference lithography and metal-assisted chemical etching. *Langmuir*, **28**(31), 11465–11471 (2012)
55. Bico, J., Thiele, U., Quere, D.: Wetting of textured surfaces. *Coll. Surf. A: Physicochem. Eng. Aspects*, **206**(1–3), 41–46 (2002)
56. Vorobyev, A.Y., Guo, C.: Laser makes silicon superwicking. *Optics & Photonics News*, December, p. 38. (2010). Video at <http://www.opnmagazine-digital.com/opn/201012/?pg=40#pg40>
57. Vorobyev, A.Y., Guo, C.: Making human enamel and dentin surfaces superwetting for enhanced adhesion. *Appl. Phys. Lett.* **99**(20), 031146 (2011)
58. Zhou, M., Yu, J., Li, J., Wu, B., Zhang, W.: Wetting induced fluid spread on structured surfaces at micro scale. *Appl. Surf. Sci.* **258**(19), 7596–7600 (2012)
59. Tuckerman, D.B., Pease, R.F.W.: High performance heat sinking for VLSI. *IEEE Electron Device Lett.* **2**(5), 126–129 (1981)
60. Stroock, A.D., Dertinger, S.K.W., Ajdari, A., Mezic, I., Stone, H.A., Whitesides, G.M.: Chaotic mixer for microchannels. *Science*, **295**(5555), 647–651 (2002)
61. Johnson, T.J., Ross, D., Locascio, L.E.: Rapid microfluidic mixing. *Anal. Chem.* **74**(1), 45–51 (2002)
62. Melin, J., Roxhed, N., Gimenez, G., Griss, P., van der Wijngaart, W., Stemme, G.: A liquid-triggered liquid microvalve for on-chip flow control. *Sens. Actuators. B.* **100**(3), 463–468 (2004)
63. Zimmermann, M., Hunziker, P., Delamarque, E.: Valves for autonomous capillary systems. *Microfluid. Nanofluid.* **5**(3), 395–402 (2008)
64. Brody, J.P., Yager, P.: Diffusion-based extraction in a microfabricated device. *Sens. Actuators A.* **58**(1), 13–18 (1997)
65. Zimmermann, M., Schmid, H., Hunziker, P., Delamarque, E.: Capillary pumps for autonomous capillary systems. *Lab Chip*, **7**, 119–125 (2007)
66. Juncker, D., Schmid, H., Drechsler, U., Wolf, H., Wolf, M., Michel, B., de Rooij, N., Delamarque, E.: Autonomous microfluidic capillary system. *Anal. Chem.* **74**(24), 6139–6144 (2002)
67. Drelich, J., Chibowski, E.: Superhydrophilic and superwetting surfaces: definition and mechanisms of control. *Langmuir*, **26**(24), 18621–18623 (2010)